Inkjet-printed Myoglobin based H_2S Sensor

KANCHANA M[1], RAJASEKARAN E[2], KUMAR B[1] AND USHA ANTONY[3]

[1]Department of Printing Technology, College of Engineering Guindy, Anna University, Chennai-600 025, Tamil Nadu, India.

[2]Department of Mechanical Engineering, College of Engineering Guindy, Anna University, Chennai-600 025, Tamil Nadu, India.

[3]College of Fish Nutrition & Food Technology, TNJFU Madhavaram Campus, Chennai- 600 051, Tamil Nadu, India.

ABSTRACT

The objective of this research work is to investigate the feasibility of fabricating bio-based visual sensor indicators to detect the presence of H_2S using inkjet printing. Myoglobin and chitosan were used as indicating and immobilizing materials respectively. 30 mg of myoglobin dissolved in 1 mL of tris buffer with 10% glycerol gave optimum jettability properties. Similarly, drop formation was optimal for 0.50% m/v chitosan solution diluted to 10 cP viscosity. The samples were fabricated in layer-by-layer approach and indicator with 2 layers of chitosan and 4 layers of myoglobin gave maximum sensitivity with 14.42 for 0.7 mg/L of H_2S. The sensors retained their functionality for 5 days even when stored at room temperature.

KEYWORDS: *Piezoelectric inkjet printing, Sensor, Myoglobin, Meat spoilage, H_2S detection.*

1.0 INTRODUCTION

Meat is a highly perishable product due to the presence of rich nutrients and high moisture content and spoilage in meat can occur due to chemical and biological activities[1,2]. Frequent power outage, lack of awareness on safe handling and storage practices may contribute to temperature fluctuations in storage of meat during transportation and distribution. Presently, consumers of meat currently have to rely only on expiry dates or use-by dates, which may not truly indicate the quality of meat inside the package[3]. The consumer confidence on the quality of packaged food and hence the brand value of the product can be increased by incorporating a sensing mechanism on the

J. Polym. Mater. Vol. **38,** No. 3-4, 2021, 309-325

Correspondence author e-mail: mani.kanchana@gmail.com
DOI : https://doi.org/10.32381/JPM.2021.38.3-4.11

package that will indicate the quality of meat inside the package at a glance [4–6]. As the market demand for packed meat is increasing, freshness indicator labels, which gives visible colour change with deterioration in meat, would be best suited for the Indian consumers. As of now, these type of intelligent packaging solutions for packaged meat products are not commercially available in India.

The potential precursors of meat spoilage are found as ethanol, acetone, ammonia, methyl ethyl ketone, biogenic amines, hydrogen sulphide, dimethyl sulphide, and carbon disulphide[7]. Among the various volatile compounds found in the headspace of the package, sulphide compounds are strongly dependent on the storage temperature and hence can be used as spoilage indicators for temperature abuse in cold chain[8]. The amount of H_2S in the headspace ranged from 3.0 to 777.1 ppb in vacuum packed chicken meat samples[9], and 1.2 mg/L to 4.7 mg/L under MAP conditions (40% CO_2, 60% N_2)[10]. Hydrogen sulphide gas level was detected from 80 to 370 mg/L in the head space when packed in Argon MAP[11]. From the above literature, it is understood that the quantities of H_2S exuded out of the meat is a good precursor for detecting the spoilage conditions. Many sensors and indicators such as semiconductor metal oxides, electrochemical sensors, optical sensors, conducting polymers and quartz crystals have been developed for industrial and packaging applications to detect H_2S[12,13]. However, these sensors are not suitable for food packaging as they require measuring instrument and utilize metal oxides or metal nanoparticles.

The current research trend is towards using renewable organic and natural bio-based materials for intelligent packaging applications[14]. Towards this, bio-based materials such as anthocyanin, chitosan and myoglobin have been used in the following research works for developing freshness indicators. Anthocyanin was blended with starch/Poly Vinyl Alcohol (PVA) solution and fabricated into a film by solution casting to detect ammonia in fish packages[15]. Aqueous chitosan solution was packed in a LDPE sachet and placed inside the package to detect the ripeness of the kimchi fruit[16]. Myoglobin solution was incorporated onto agar gels to detect H_2S in meat packaging[10]. Nevertheless, most of these experimental prototypes require further development for commercial applications due to inherent lacunae in the fabrication process.

The reaction of H_2S with the proteins found in living organisms such as cytochrome c oxidase, haemoglobin, myoglobin and ferritin is extensively documented[17–20]. The reaction of H_2S with myoglobin leads to formation of irreversible greenish compounds called sulfmyoglobin in the presence of O_2. It is used in biosensors as receptors to sense the target analytes[21]. Therefore, utilizing myoglobin as H_2S indicators would be feasible and is compatible for food packaging applications. Direct deposition of protein on packaging material may lead to decline in its activity and proteins are generally immobilized in organic or inorganic materials to provide thermal and physical stability[22]. Chitosan, a linear polysaccharide, obtained from deacetylation of chitin is one of the extensively used materials

in biosensor applications due to its excellent film forming ability, permeability, optical transparency and capacity to physically entrap and chemically immobilize bio-molecules[23]. Hence, chitosan was selected to immobilize the proteins.

Inkjet printing offers accurate patterning, controlled deposition, repeatability, productivity and cost effectiveness and it has been used for fabrication of biosensors using many proteins[24–26]. Even though, it has been used to deposit proteins in biosensor applications, inkjet printing of myoglobin has not been documented. Therefore, in this research work, it is proposed to fabricate and analyse the performance of myoglobin based sensor with chitosan as immobilizing layer using layer-by-layer approach in inkjet printing that would make it feasible for large scale production. Myoglobin and chitosan were formulated into jettable liquids and the printability parameters were optimized. The sensors were evaluated for their colour change on exposure to varying concentration of H_2S and shelf life studies for a period of 5 days.

2.0 MATERIALS

Low molecular weight chitosan (viscosity 20-300 cP in 2% acetic acid) was purchased from CDH, India. Myoglobin (essentially salt-free, lyophilized powder) and tris buffered saline (pH 8.0) were purchased from Sigma Aldrich, India. Broken ferrous sulphide pellets, HCl, acetic acid glacial and glycerol were purchased from Merck, India.

3.0 METHODS

3.1 Ink Formulation

The chitosan stock solution (0.50% m/v) was prepared by mixing 0.25 g of chitosan in 50 mL of 1% acetic acid. The stock solution was diluted with 1% acetic acid solution to three different viscosity levels: 5 cP (CH-05), 10 cP (CH-10) and 15 cP (CH-15).

The tris buffer solutions with different concentrations of glycerol (0–30% v/v) were tested in the inkjet printer prior to the addition of myoglobin to find out the optimum proportion that gives good jettability without blocking of nozzles. Then myoglobin was dissolved to this buffer solution (MB) in the ratio of 30 mg/mL.

3.2 Ink Characterization

The rheology of the solutions was measured using a cone and plate rheometer (Anton Paar MCR 302 Rheometer, USA). Interfacial contact angle of the solutions was measured in contact angle meter (Holmarc, India) using sessile drop method. The surface tension values were calculated using Pendant Drop plugin, in Image J FIJI software.

3.3 Inkjet Printing Characterization

Jetlab 4XL drop-on-demand piezoelectric inkjet printer (Microfab, USA) was used to deposit the inks. Bipolar waveform is used to control the droplet ejection. The liquid to be printed was filtered with 0.22 µm Whatman PVDF syringe filter. The drop formation and the trajectory of the drop were observed by the Navitar camera in the printer. Aphelion image analysis software was used to find out the jetting velocity, drop volume and drop diameter. The fabricated sensors were characterized for their roughness and thickness in the Talysurf non-contact surface roughness tester.

3.4 Sensor Fabrication

The base layer of chitosan was printed in different spacing in the X and Y direction to identify the resolution that would give a uniform immobilizing surface. After identifying the resolution for myoglobin layer in a similar manner, myoglobin was printed in varying number of layers from 1 to 4 (M1, M2, M3, M4) above 2 layers of chitosan (C1, C2) to produce a freshness indicator that would give visible colour difference on reacting with H_2S. The dimensions of the printed features were measured using Nexius Stereo Zoom Microscope or Olympus phase contrast microscope.

3.5 Sensor Analysis

As discussed in the section 1.0, varying amount of H_2S

gas was emitted in meat packages according to the type of meat, processing conditions, storage temperature and type of packaging. In the experimental work carried out by Smolander and other coworkers, myoglobin sensor prepared by pipetting myoglobin solution in the agarose gel were tested for H_2S sensitivity by varying the gas concentration from 0.0 mg/L to 2.8 mg/L [10].

In the present work also, the same range of gas concentration in four different levels (0.7 mg/L, 1.4 mg/L, 2.1 mg/L or 2.8 mg/L) was taken to evaluate the freshness indicators. The indicators (M1, M2, M3, M4) were exposed to H_2S gas in an airtight glass container (Duran® pressure plus bottles, Sigma Aldrich) of volume 180 mL fitted with Duran® GL 45 connection system cap. The required amount of H_2S gas was injected into the bottle using a 1 mL SGE gas tight syringe and the indicators were exposed to H_2S atmosphere for a duration of one hour. The colour values of the indicators before and after exposure to H_2S were evaluated using Spectrodens Premium (Techkon, Germany). The colour difference in the indicators were calculated using the equation:

$$\Delta E = [(L_1^* - L_2^*)^2 + (a_1^* - a_2^*)^2 + (b_1^* - b_2^*)^2]^{1/2}$$

where L_1^*, a_1^*, b_1^* are reference colour values and L_2^*, a_2^*, b_2^* are the sample colour values.

For evaluating the shelf life of the indicators, 5 samples were stored in room condition (25°C ± 1°C) and the sensitivity to H_2S gas was tested for 5 consecutive days. The spectral reflectance and CIE LAB values were measured under M0 conditions for all the samples.

4.0 RESULTS AND DISCUSSION

4.1 Chitosan Ink Characterization

The physiochemical properties of the chitosan solutions are tabulated in Table 1. Density values increased marginally with increase in concentration while the surface tension of the chitosan solution was found to be marginally decreasing with increase in viscosity. Lower surface tension increases drop spreading on contact with the substrate and vice versa. Also, lower surface tension inks could lead to uptake of air in-between the droplets and formation of satellite drops A similar behaviour for chitosan and its derivatives was observed by Blanco and coworkers and they attributed the reason as increasing polymer presence at the air/liquid interface [27]. Similar results were also reported by Kuo, T. Y. and coworkers and Payet & Terentjev [28,29]. The shape of the printed pattern is highly dependent on the contact angle. The contact angle of the chitosan solutions was less than 25° implying good wettability properties. The contact angle of the chitosan solutions increased slightly with increase in viscosity as reported by El-Helfian and coworkers [30].

TABLE 1. Physiochemical properties of chitosan solution

Solution	Viscosity (cP)	Density (g/cm^3)	Surface Tension (dynes/cm)	Contact angle (°)
CH-5	4.98	1.002	70.33	16.54
CH-10	10.15	1.008	64.05	18.50
CH-15	15.05	1.014	60.18	21.03
CH-20	20.28	1.021	55.13	24.16

Figure 1 shows the rheological behaviour of the chitosan solutions at different viscosities. For

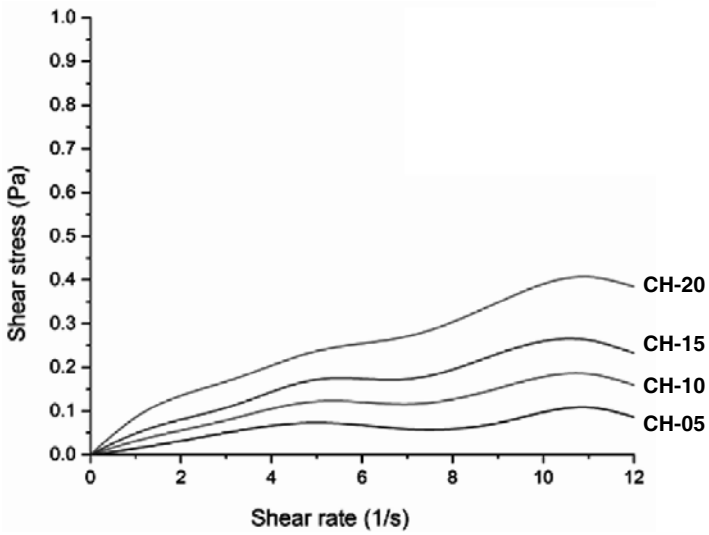

Figure 1. Rheology of chitosan solutions

a constant shear rate, the shear stress increases with the viscosity of the solution. As the viscosity increases, the increase in shear stress with increase in shear rate was more prominent. From the graph, it could be inferred that the chitosan solution exhibits pseudoplastic non-Newtonian behaviour which is similar to the results obtained in the work carried out by El-Helfian and et al.,[31]. For non-newtonian fluids, pinching of liquid from the liquid column, thinning of the ligament without breaking and retraction of the liquid into a spherical drop in inkjet printing is governed by the inertial and viscoelastic forces of the polymer chains.

4.2 Myoglobin Ink Characterization

Myoglobin in tris buffer tends to dry in the tip of the nozzle and hence, glycerol was added as humectant. The physiochemical and jettability properties of tris buffer solution with different percentages of glycerol are shown in Table 2. Consistent jetting without any blocking of nozzle was observed when glycerol percentage was 10%. Hence, 30 mg of myoglobin was dissolved in 1 mL of tris buffer with 10% v/v glycerol.

The formulated myoglobin had viscosity and surface tension within the specified range of the printer. The low contact angle values of the solution on the glass surface indicates good wettability. However, the contact angle measured on printed chitosan surface showed a significant increase. This could be attributed to the surface energy and roughness of the chitosan layer. Figure 2 indicates the Newtonian behaviour of the myoglobin solution. The increasing shear rate had a negligible influence on the shear stress of the solution. In Newtonian fluids, the drops have no ligament formation after separation of drop from the liquid column.

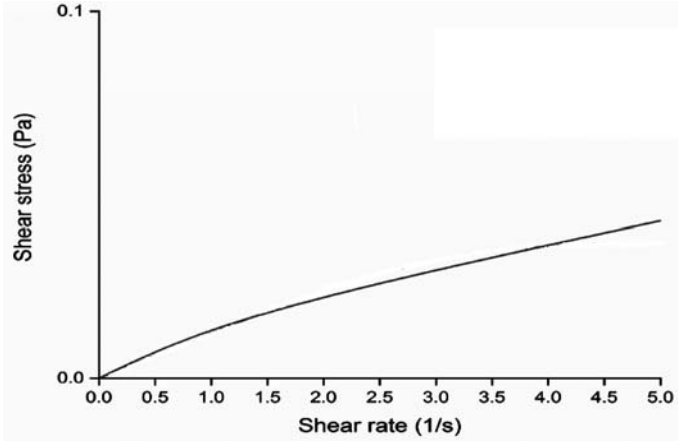

Figure 2. Rheology of myoglobin solution

TABLE 2. Physiochemical and jettability properties of myoglobin

Solution	Glycerol (% v/v)	Density (g/cm^3)	Viscosity (cP)	Surface Tension (dynes/ cm)	Contact angle on glass (°)	Contact angle on printed chitosan pattern (°)	Drying in nozzle	Jettability
Tris buffer	0	1.0045	1.81	50.28	26.7	—	Yes	Spraying
	1	1.0093	1.84	50.28	26.4	—		
	5	1.0259	1.96	50.27	25.2	—		Good
	10	1.0684	2.09	50.21	21.2	—	No	
	20	1.0759	2.39	49.96	18.7	—		
	30	1.0981	2.44	49.68	16.3	—		
Myoglobin (30 mg/ml in tris buffer)	10	1.0812	2.95	50.84	9.15	67.73		

4.3 Jettability

4.3.1 Waveform parameters

In addition to the physiochemical properties of the jetting liquid, the formation of drops is influenced by the shape of the waveform applied to actuate the print head. The jetting waveform parameters and the corresponding droplet attributes are tabulated in Table 3. For chitosan solutions, jetting voltage (Dwell voltage) required to detach the droplet from the nozzle increased with increase in viscosity of the solutions as higher voltages are required to cause larger deflections sufficient to eject the high viscosity liquids[32]. The print head height was kept at 1.00 mm from the substrate for CH-05 and

TABLE 3. Optimized waveform parameters

Solution	Rise time 1 (µs)	Dwell time (µs)	Fall time (µs)	Echo time (µs)	Rise time 2 (µs)	Idle Voltage (V)	Dwell Voltage (V)	Echo Voltage (V)	Frequency (Hz)	Vacuum level (kPa)	Print head height (mm)	Drop velocity (m/s)	Drop volume (pL)	Drop diameter (µm)
CH-05	4	25	8	25	4	0	28	-28	500	2.0	1.00	1.80	262.0	79.42
CH-10	3	29	4	56	3	0	29	-29	500	2.4	1.20	2.27	274.0	80.65
CH-15	3	24	4	40	3	0	30	-30	500	2.8	1.30	2.66	334.0	86.68
MB	21	28	10	40	23	0	27	27	300	2.8	1.00	1.59	286.8	81.82

gradually increased for the higher viscosity solutions to accommodate the increase in ligament length. The drop volume and drop diameter increased consistently for CH-05 to CH-15 due to the increase in jetting voltage[32].

4.3.2 Jetting consistency

After optimising the waveform parameters, jetting consistency was observed by measuring the drop volume and drop diameter in 5 minutes interval for a duration of 30 minutes. The results for chitosan solutions and myoglobin are tabulated in Table 4. Frequent nozzle blocking was encountered for CH-15 solutions. Chitosan solution with maximum of 10 cP viscosity could be printed without nozzle blocking issues. Hence, CH-10 formulation was chosen for printing the base immobilizing layer. The MB solution had consistent jetting with variation in drop diameter within 3 µm and didn't have nozzle blocking issues.

4.4 Morphological Analysis

The sensors were fabricated in square pattern using layer-by-layer technique with chitosan as base immobilizing layer, over which myoglobin was printed as indicator layer. For forming the immobilization layer, CH-10 solution was jetted as individual dots and the dot diameters were measured. The mean dot diameter was found to be 0.302 mm (SD – 0.010 mm) along X axis and 0.286 mm (SD – 0.008 mm) along Y axis. The variations in the dot diameter can be attributed to the inertial force, viscoelastic property of the fluid and surface energy of the substrate[33]. The optimum spacing required between individual dots to coalesce together to produce a continuous line was determined by forming lines with decreasing dot spacing from 0.14 mm to 0.11 mm in the X direction [Fig. 3(a)]. On close observation, 'stacked coin appearance' of the jetted drops [Fig. 3(b)] was visible which indicates immediate drying of the chitosan at the drop edges before the next drop was jetted[34]. At drop spacing of 0.11 mm, a uniform line pattern was obtained and the observed line patterns were similar to the results obtained in[33–35]. Similarly, the optimum drop spacing in the Y direction was determined

TABLE 4. Drop Stability Observations

Time (min)	CH-05			CH-10			CH-15			MB		
	Drop velocity (in m/s)	Drop volume (in pL)	Drop diameter (in µm)	Drop velocity (in m/s)	Drop volume (in pL)	Drop diameter (in µm)	Drop velocity (in m/s)	Drop volume (in pL)	Drop diameter (in µm)	Drop velocity (in m/s)	Drop volume (in pL)	Drop diameter (in µm)
0	1.87	262.3	79.42	2.27	274.6	80.65	2.66	331.0	85.83	1.87	262.3	79.42
5	1.92	241.9	77.31	2.24	270.9	80.28	2.61	314.4	84.37	1.88	261.9	79.38
10	1.8	328.7	85.62	2.16	276.0	80.78	2.56	320.1	84.87	1.80	275.3	80.68
15	1.80	271.0	80.28	2.17	273.2	80.50	2.51	306.2	83.62	1.80	282.0	81.36
20	1.85	250.9	78.25	2.15	269.0	80.09	2.48	310.3	83.99	1.85	270.9	80.26
25	1.86	341.7	86.74	2.15	271.8	80.37	2.43	311.7	84.12	1.86	283.7	81.52
30	1.96	334.9	86.16	2.17	270.4	80.23	2.41	313.3	84.27	1.86	264.9	79.68

to be 0.15 mm [Fig. 3(c)]. Two layers of chitosan (C1, C2) were printed in the shape of a 5 mm x 5 mm square with layer pattern as showed in Figure 3(d).

The mean diameter of the myoglobin printed dot was found to be 0.261 mm (SD – 0.019 mm) along X axis and 0.217 mm (SD – 0.016 mm) along Y axis. Unlike chitosan, initial trials with myoglobin implied that drops coalesced in both X and Y direction. Hence, it was decided to keep uniform drop spacing in the X and Y direction for forming the myoglobin layer. The drop spacing was decreased from 0.12 mm to 0.07 mm [Fig. 4(a)] and the optimum drop spacing was found to be 0.08 mm as it gave a uniform pattern. The freshness indicators of varying colour saturation were fabricated by increasing the number of layers from 1 to 4 namely M1, M2, M3 and M4 [Fig. 4(b)]. The drop spacing and layer pattern were kept identical for all the layers.

The 3D surface profile of the printed layers are shown in Figure 5. From the morphological parameters listed in Table 5, it could be observed that double layer chitosan has a smoother surface than the single layer validating the selection of double layer of chitosan as the base layer. In myoglobin layers, the average roughness increases with number of layers except for M4. The height of the layers is measured by drawing a line profile across the unprinted surface and the printed layers and calculating the height difference in the profile. The thickness values show a clear increasing trend with increase in number of layers.

4.5 Spectral Analysis

The spectral reflectance of the myoglobin based indicators is shown in Figure 6 and the colour values of the indicators are listed in Table

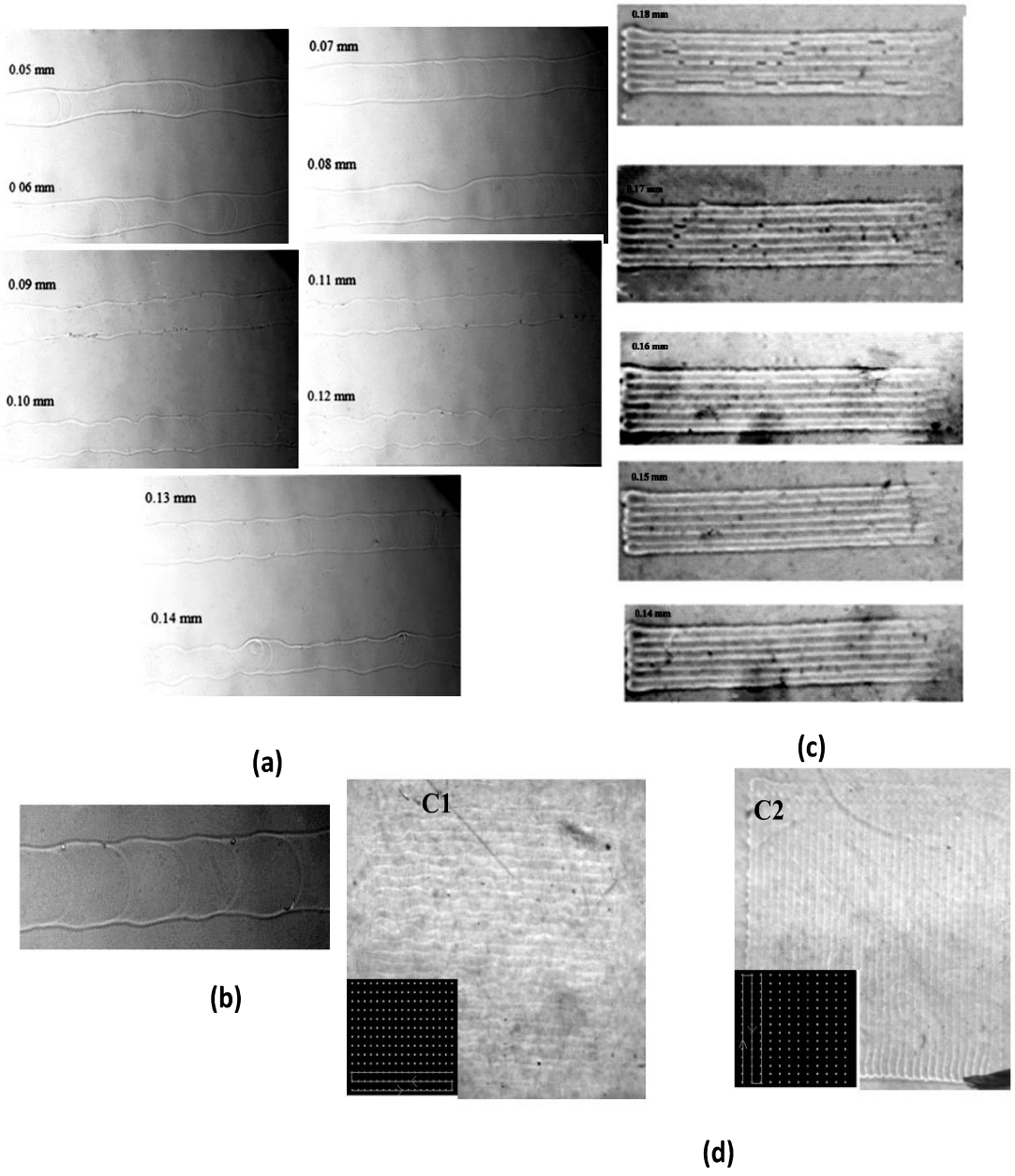

Figure 3. Printing of chitosan (a) Varying x spacing; (b) Stacked coin appearance; (c) Varying y spacing; (d) Single layer and double layer patterns

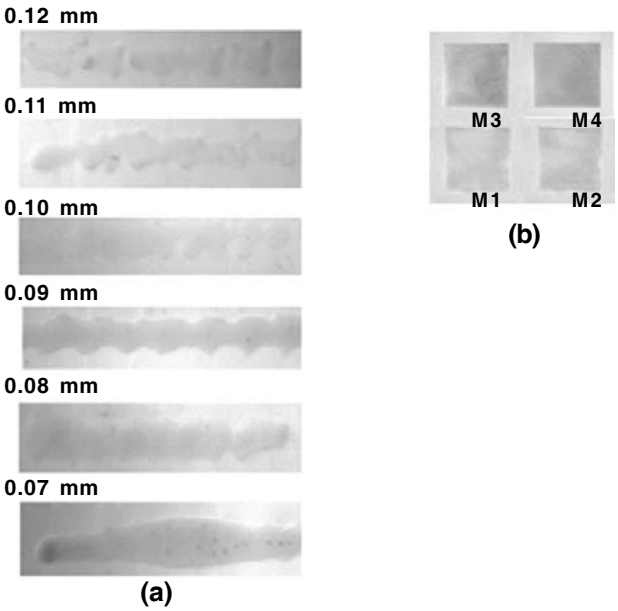

Figure 4. (a) Myoglobin lines with various drop spacing; (b) Myoglobin based sensor

TABLE 5. Roughness and thickness values of printed layers

Print Patterns	Average layer roughness R_a (in µm)	Thickness (in µm)
C1	0.024	0.377
C2	0.015	0.757
M1	0.124	1.896
M2	0.145	2.226
M3	0.159	2.341
M4	0.155	3.028

6. It is observed that the overall reflectance (L*) of the indicators decreased with increase in number of layers. The increase in b* values implies increase in saturation of yellowness of the samples. However, the colour difference between the subsequent layers significantly decreased between M3 and M4.

4.6 Functional Analysis

The spectral reflectance curves of the freshness indicators after exposure to H_2S were plotted in Figure 7(a). The change in the spectral reflectance increased with increase in the number of layers and concentration of H_2S. Hence, it can be inferred that myoglobin when immobilized on chitosan using inkjet printing technology retains its functionality. The colour difference on exposure to varying concentrations of H_2S are listed in Table 7 and the image of indicators before and after

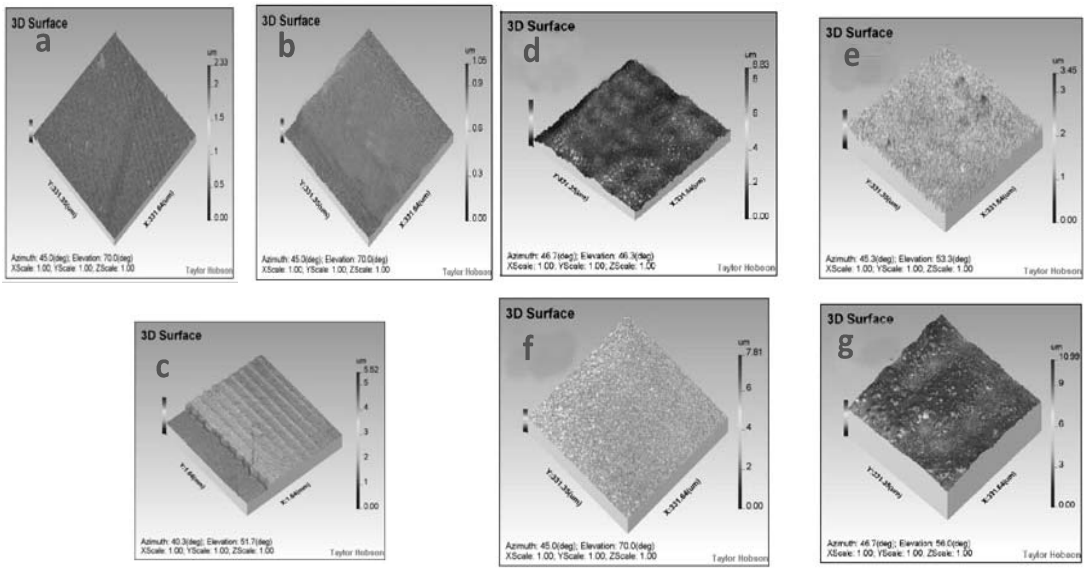

Figure 5. 3D profile of printed layers (a) C1 layer (b) C2 layer (c) C2 thickness profile (d) M1 layer (e) M2 layer (f) M3 layer (g) M4 layer

exposure to H_2S is shown in Figure 7(b). The response of the indicators was promising as it was observed that even for the single layer myoglobin based indicator (M1), ΔE was 7.24 when it was exposed to the least concentration of H_2S of 0.7 mg/L.

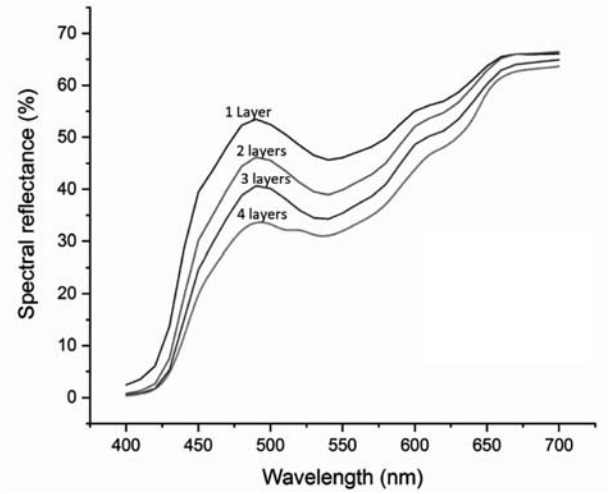

Figure 6. Spectral reflectance of myoglobin based freshness indicators

TABLE 6. Colour values of myoglobin based indicators before exposure

Sample name	L*	a*	b*	ΔE (Reference: M1)
M1	76.15	2.34	14.37	—
M2	72.77	5.63	19.52	**5.13**
M3	69.81	7.60	21.85	**11.13**
M4	66.53	8.31	23.20	**14.08**

Generally, ΔE of greater than 5.0 implies a significant visible colour difference to a human observer. However, ΔE remained nearly the same for M1, with increase in H2S concentration indicating that the amount of myoglobin available for reaction was insufficient. The ΔE values were significantly higher for M2, M3 and M4 when the gas concentration was increased.

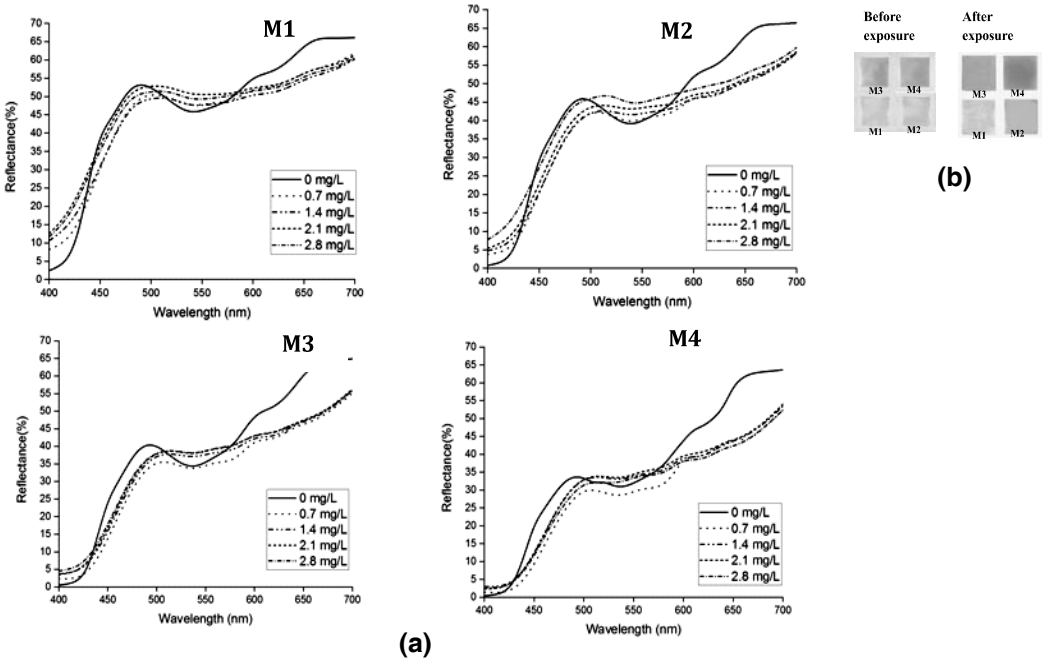

Figure 7. (a) Spectral reflectance of myoglobin based sensors on exposure to H_2S; (b) Colour change of the indicators

The ΔE value obtained for 1.4 mg/L and 2.8 mg/L of H_2S concentrations for the agarose based myoglobin indicators prepared by Smolander and coworkers were 7.4 and 5.6 respectively[10]. For the same amount of concentration, the ΔE values obtained for inkjet

printed myoglobin based freshness indicators were 16.47 and 17.28 respectively. The increased sensitivity of the inkjet printed myoglobin based indicators can be attributed to the thin chitosan immobilizing layer of 0.757 µm compared to the 2 mm agarose gel used by Smolander and coworkers. Also, in their work, myoglobin was dissolved in sodium phosphate buffer, whereas in the present work 10% of glycerol was added to the tris buffer in formulating myoglobin solution. The presence of glycerol also contributed towards the increased sensitivity of myoglobin.

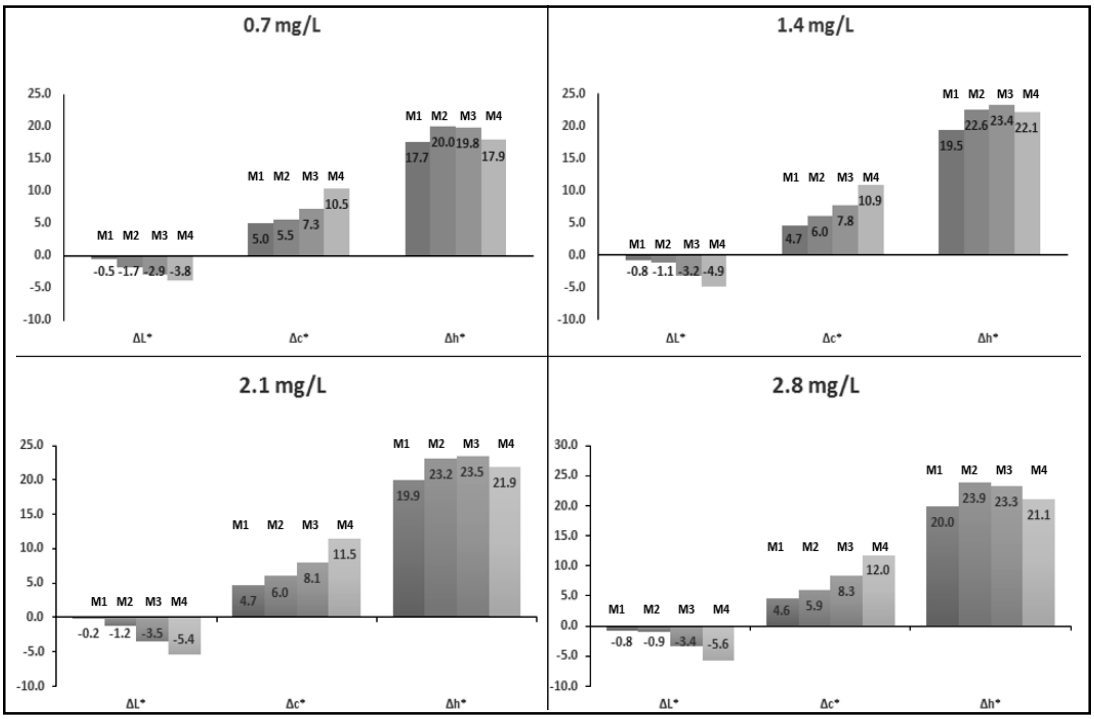

Figure 8. Colour difference in myoglobin based sensors

TABLE 7. Colour values of myoglobin based indicators on exposure to H_2S

H_2S concentration (mg/L)	Colour difference (ΔE)			
	M1	M2	M3	M4
0.7	7.24	9.89	12.04	14.42
1.4	7.40	10.95	13.70	16.47
2.1	7.44	11.12	14.02	17.04
2.8	7.45	11.28	14.10	17.28

The change in ΔL*, Δc* and Δh* for M1, M2, M3 and M4 are plotted in Figure 8. For M1 and M2, ΔL* was negligible even though the overall colour difference was significant. The change in chroma Δc*, showed an increasing trend with increase in layers while the change in hue Δh* was in increasing trend for M1, M2 and M3 while it dropped a little for M4. The visual perception of colour change on exposure to H_2S will be significant as the change in hue is maximum.

4.7 Shelf Life

Five samples of myoglobin based sensors (M4A, M4B, M4C, M4D and M4E) were fabricated for shelf life analysis. The colour values of the indicators were tabulated in Table 8. The colour difference value between the samples were less than 2.0 which indicates good repeatability. The ΔE value calculated with Sample M4A as reference value ranged from 1.32 to 1.85 which implies indistinguishable

TABLE 8. Colour values of myoglobin based freshness indicators for shelf life evaluation

Sample	**Colour values**	**M4A**	**M4B**	**M4C**	**M4D**	**M4E**
H_2S concentration (mg/L)		Day_1	Day_2	Day_3	Day_4	Day_5
0	L*	66.86	68.49	67.73	66.25	67.10
	a*	8.94	8.31	8.03	7.85	7.98
	b*	23.28	23.88	22.55	23.71	22.20
ΔE between samples (Ref:M4A)			**1.85**	**1.46**	**1.32**	**1.46**
			ΔE (Ref: M4A)			
0.7	L*	64.21	1.30	1.50	1.51	0.88
	a*	1.81				
	b*	35.55				
1.4	L*	61.85	2.05	1.52	0.76	2.69
	a*	-0.77				
	b*	35.93				
2.1	L*	61.74	2.22	1.37	1.31	1.52
	a*	-0.53				
	b*	36.25				
2.8	L*	61.22	1.76	1.66	1.81	1.75
	a*	-0.29				
	b*	37.11				

colour difference among the samples. All these indicators were stored at 23°C and one sample was taken every day for testing sensitivity to H_2S. The colour change of all the sensors on exposure to different concentrations of H_2S were similar. Most of the ΔE values between the reacted indicators tested on different days were less than 2.5 and only one sample had ΔE value of 2.69. These results indicate that the myoglobin based freshness indicators were functionally active for the entire duration of 5 days even when kept at room temperature (25°C $\pm$ 1°C) which is higher than the normal storage temperature (4°C $\pm$ 1°C) and temperature abuse conditions (14°C $\pm$ 1°C) for the chilled meat packages.

5.0 CONCLUSION

A biobased sensor that shows visual colour change on reaction with H_2S has been developed in this research work. Piezoelectric inkjet based printing utilizing layer-by-layer approach was used to immobilize the myoglobin on chitosan base layer. The waveform parameters, drop spacing and layer pattern for chitosan and myoglobin were determined. The fabricated sensors exhibited significant colour change on exposing to different concentrations of H_2S. The colour difference was maximum for the four-layer structure, with sensitivity from 14.42 to 17.28 and displayed stable functionality for a period of 5 days when stored at room temperature. Overall, the result of the research work implies that piezoelectric inkjet printing can be used for fabrication of the myoglobin based freshness indicators successfully. As future work, the sensor/indicator can be fabricated using industrial inkjet printing heads that are directly fitted in the meat packaging production line so as to fabricate the indicators onto the packaging materials just before sealing the packages.

ACKNOWLEDGEMENT

The authors are grateful to the Department of Biotechnology, Ministry of Science and Technology, Government of India for funding the project.

REFERENCES

1. Addis, M. (2015). Major Causes Of Meat Spoilage and Preservation Techniques: A Review. *Food Science and Quality Management,* 41, 2224–6088. www.iiste.org
2. Kanchana, M., Jayappriyan, R. M., Kumar, B., & Antony, U. (2017). Investigation of Formability, Morphology and Functionality of Chitosan based Biosensors. 34(4), 797–808.
3. Lewis, C. (2002). Food Freshness and "Smart" Packaging (p. Vol 36,No. 5). FDA Consumer magazine, U.S. Food and Drug Administration. https://permanent.access.gpo.gov/lps1609/www.fda.gov/fdac/features/2002/502_ food.html
4. Ghaani, M., Cozzolino, C. A., Castelli, G., & Farris, S. (2016). An overview of the intelligent packaging technologies in the food sector. *Trends in Food Science & Technology,* 51, 1–11.
5. Restuccia, D., Spizzirri, U. G., Parisi, O. I., Cirillo, G., Curcio, M., Iemma, F., Puoci, F., Vinci, G., & Picci, N. (2010). New EU regulation aspects and global market of active and intelligent packaging for food industry applications. *Food Control,* 21(11), 1425-1435.
6. Fortin, C., Goodwin, H. L., & Thomsen, M. (2009). Consumer Attitudes toward Freshness Indicators on Perishable Food Products. *Journal of Food Distribution Research,* 40(3), 1–15.
7. Nychas, G. J. E., Skandamis, P. N., Tassou, C. C., & Koutsoumanis, K. P. (2008). *Meat spoilage* during distribution. *Meat Science*, 78(1–2), 77–89.

8. Komitopoulou, E. (2012). Microbial and chemical markers of. *International Meat Topics,* 3(3).

9. Senter, S. D., Arnold, J. W., & Chew, V. (2000). APC values and volatile compounds formed in commercially processed, raw chicken parts during storage at 4 and 13??C and under simulated temperature abuse conditions. *Journal of the Science of Food and Agriculture,* 80(10), 1559–1564.

10. Smolander, M., Hurme, E., Latva-Kala, K., Luoma, T., Alakomi, H.-L., & Ahvenainen, R. (2002). Myoglobin-based indicators for the evaluation of freshness of unmarinated broiler cuts. *Innovative Food Science & Emerging Technologies,* 3(3), 279–288.

11. Tománková, J., Boøilová, G., Steinhauserová, I., & Gallas, L. (2012). Volatile Organic Compounds as Biomarkers of the Freshness of Poultry Meat Packaged in a Modified Atmosphere. 30(5), 395–403.

12. Pandey, S. K., Kim, K., & Tang, K. (2012). A review of sensor-based methods for monitoring hydrogen sulfide. *Trends in Analytical Chemistry,* 32.

13. Zhai, X., Li, Z., Shi, J., Huang, X., Sun, Z., Zhang, D., Zou, X., Sun, Y., Zhang, J., Holmes, M., Gong, Y., Povey, M., & Wang, S. (2019). A colorimetric hydrogen sulfide sensor based on gellan gum-silver nanoparticles bionanocomposite for monitoring of meat spoilage in intelligent packaging. *Food Chemistry,* 290, 135–143.

14. Ahmed, I., Lin, H., Zou, L., Li, Z., Brody, A. L., Qazi, I. M., Lv, L., Pavase, T. R., Khan, M. U., Khan, S., & Sun, L. (2018). An overview of smart packaging technologies for monitoring safety and quality of meat and meat products. *Packaging Technology and Science,* 31(7), 449-471.

15. Zhai, X., Shi, J., Zou, X., Wang, S., Jiang, C., Zhang, J., Huang, X., Zhang, W., & Holmes, M. (2017). Novel colorimetric films based on starch/ polyvinyl alcohol incorporated with roselle anthocyanins for fish freshness monitoring. *Food Hydrocolloids,* 69, 308-317.

16. Jung, J., Lee, K., Puligundla, P., & Ko, S. (2013). Chitosan-based carbon dioxide indicator to communicate the onset of kimchiripening. LWT - *Food Science and Technology,* 54(1), 101–106.

17. Li, Q., & Lancaster, J. R. (2013). Chemical foundations of hydrogen sulfide biology. *Nitric Oxide - Biology and Chemistry,* 35(August 2014), 21–34.

18. Ríos-gonzález, B. B., Román-morales, E. M., Pietri, R., & López-garriga, J. (2014). Hydrogen sul fi de activation in hemeproteins/ : The sulfheme scenario. *Journal of Inorganic Biochemistry,* 133, 78–86.

19. Román-morales, E., Pietri, R., Ramos-santana, B., Vinogradov, S. N., Lewis-ballester, A., & López-garriga, J. (2010). Biochemical and Biophysical Research Communications Structural determinants for the formation of sulfhemeprotein complexes. 400, 489–492.

20. Boubeta, F. M., Bieza, S. A., Bringas, M., Estrin, A., Boechi, L., & Bari, S. E. (2018). Mechanism of Sulfide Binding by Ferric Hemeproteins, *Inorganic Chemistry,* 2;57(13):7591-7600.

21. Vilian, A. T. E., Veeramani, V., Chen, S. M., Madhu, R., Kwak, C. H., Huh, Y. S., & Han, Y. K. (2015). Immobilization of myoglobin on Au nanoparticle-decorated carbon nanotube/polytyramine composite as a mediator-free H2O2 and nitrite biosensor. *Scientific Reports,* 5(1), 1–10.

22. Dave, B. C., Miller, J. M., Dunn, B., Valentine, J. S., & Zink, J. I. (1997). Encapsulation of Proteins in Bulk and Thin Film Sol-Gel Matrices. *Journal of Sol-Gel Science and Technology,* 8(1-3), 629–634.

23. Kanchana, M., Jayappriyan, R. M., Kumar, B., & Antony, U. (2017). Investigation of Formability, Morphology and Functionality of Chitosan based Biosensors. 34(4), 797–809.

24. Delaney, J. T., Smith, J., & Schubert, U. S. (2009). Inkjet printing of proteins. *Soft Matter,* 24, 4866–4877.

25. Hasenbank, M. S., Edwards, T., Fu, E., Garzon, R., Kosar, T. F., Look, M., Mashadi-Hossein, A., & Yager, P. (2008). Demonstration of multi-analyte patterning using piezoelectric inkjet printing of multiple layers. *Analytica Chimica Acta,* 611(1), 80–88.

26. Newman, J. D., Turner, A. P. F., & Marrazza, G. (1992). Ink-jet printing for the fabrication of amperometric glucose biosensors. *Analytica Chimica Acta,* 262(1), 13–17.

27. Blanco, A., García-Abuín, A., Gómez-Díaz, D., & Navaza, J. M. (2013). Physicochemical characterization of chitosan derivatives. CyTA - *Journal of Food,* 11(2), 190–197.

28. Kuo, T. Y., Jhang, C. F., Lin, C. M., Hsien, T. Y., & Hsieh, H. J. (2017). Fabrication and application of coaxial polyvinyl alcohol/chitosan nanofiber membranes. *Open Physics,* 15(1), 1004–1014.

29. Payet, L., & Terentjev, E. M. (2008). Emulsification and stabilization mechanisms of O/W emulsions in the presence of chitosan. *Langmuir,* 24(21), 12247–12252.

30. El-Hefian, E. a., Nasef, M. M., & Yahaya, A. H. (2010). Preparation and Characterization of Chitosan/Polyvinyl Alcohol Blends-A Rheological Study. *E-Journal of Chemistry,* 7(s1), S349–S357.

31. El-Hefian, E. A., Elgannoudi, E. S., Mainal, A., & Yahaya, A. H. (2010). Characterization of chitosan in acetic acid: Rheological and thermal studies. *Turkish Journal of Chemistry,* 34(1), 47–56.

32. Roberto Bernasconi, Stefano Brovelli, Prisca Viviani, Marco Soldo, Domenico Giusti, L. M. (2021). Adv Eng Mater - 2021 - Bernasconi - Piezoelectric Drop On Demand Inkjet Printing of High Viscosity Inks.pdf. *Advanced Engineerig Materials,* 2100733 (1-14).

33. Derby, B. (2010). Inkjet Printing of Functional and Structural Materials: Fluid Property Requirements, Feature Stability, and Resolution. *Annual Review of Materials Research*, *40*(1), 395–414.

34. Soltman, D., & Subramanian, V. (2008). Inkjet-Printed Line Morphologies and Temperature Control of the.pdf. *Langmuir/ : The ACS Journal of Surfaces and Colloids*, *24*(5), 2224-2231.

35. Stringer, J., & Derby, B. (2009). Limits to feature size and resolution in ink jet printing. *Journal of the European Ceramic Society*, *29*(5), 913–918.

Received: 31-03-2021

Accepted: 16-09-2021